JOURNAL OF APPLIED ELECTROCHEMISTRY **27** (1997) 462–468

Effect of gelling on the surface structure of a porous lead electrode in sulfuric acid

M. P. VINOD, A. B. MANDLE, S. R. SAINKAR, K. VIJAYAMOHANAN

Physical Chemistry Division, National Chemical Laboratory, Pune 411 008, India

Received 3 June 1996; revised 27 August 1996

Effect of immobilizing the electrolyte using thixotropic agents such as sodium silicate on the electrochemical behaviour of lead in sulfuric acid is studied using electrochemical methods such as cyclic voltammetry (CV), charging curve technique, Tafel polarization and surface spectroscopic methods including X-ray photoelectron spectroscopy (XPS) and scanning electron microscopy (SEM). CV studies indicate a 700 mV cathodic shift in the hydrogen evolution potential as a result of gelling while the well-known reversible Pb/Pb^{2+} couple is found to be thermodynamically disfavoured (100 mV and 50 mV shifts for the Pb dissolution and Pb^{2+} reduction reactions respectively). In addition, a significant change in the double layer capacitance by 600 $\mu F\ cm^{-2}$ is observed at the same potential probably due to the contribution of silicate adsorption at the interfacial region. Exchange current density values for hydrogen evolution reaction calculated from Tafel plots are 1.35×10^{-6} A cm^{-2} and 1.31×10^{-8} A cm^{-2} for free and gelled electrolytes, respectively, which reveal the kinetic suppression of HER. However, XPS studies give no evidence for the chemisorption of silicate on the lead surface, although SEM analysis shows appreciable change in the surface morphology.

1. Introduction

Gels provide a unique environment which cannot be envisaged by their parent solid or liquid components from which they are generally derived [1]. Use of gels as media for chemical reactions provides a unique way of controlling nucleation, growth, and any type of phase transitions during the reactions, by regulating the viscosity. Both organic and aqueous types of gels are currently used for several chemical, physical and biological applications. For example, electrically erodable polymeric gels are used for controlled-drug delivery systems [2] and also for understanding certain intermolecular interactions [3]. Gelled systems are also successfully used for diffusion limited aggregation in a wide range of phenomena such as electrodeposition [4], random dendritic growth [5], fluid–fluid displacement in porous media [6], dielectric breakdown [7] and for biological process such as the growth of nerve cells and blood vessels [8]. Yet another application is in catalysis where, mixed metal oxides such as vanadium silicate xerogels are prepared and tested for specific catalytic activity for reactions like alkene oxidation [9].

These gelled systems are also found to offer several advantages in electrochemical applications [10, 11]. They can be used either to immobilize an electroactive substance at an electrode surface or as a polymer electrolyte itself. Gels are particularly suitable for electrochemical systems where dimensional changes occur on the electrode as a result of electrochemical reactions including dissolution–precipitation processes since they are deformable and can accommodate such volume changes. In addition, gels of silica and transition metal hydroxides are appropriate media for performing electrochemistry due to the high content of free solvent. Therefore, it was a natural development of such studies to prepare modified electrodes from these gels. For instance, in a recent study, glucose oxidase was incorporated along with a water sol using ferrocene as a mediator in silica gels and its electrocatalytic activity was studied by following the electrochemistry of ferrocene [12].

One specific application of gels in electrochemical systems is in sealed maintenance-free (MF) lead–acid batteries [13, 14], where the electrolyte is immobilized with organic or inorganic thixotropic agents [15]. The original reason for immobilizing the electrolyte was to avoid acid spillover from batteries, especially under stringent conditions like that in an aircraft. Subsequently, it was observed that due to the partial drying out, such gels exhibit improved gas recombination characteristics. These gelled systems do not require periodic topping up of the electrolyte for two main reasons: the amount of hydrogen produced is less compared to the flooded electrolyte and, more importantly, the oxygen released at the positive electrode migrates to the negative through cracks in the gelled electrolytes leading to recombination with the highly active lead surface. Thus, the electrolyte loss is negligible in gelled electrolyte systems. These types of gelled batteries are found to be especially suitable for severe duty such as remote area power supplies (RAPS) where a well defined charging regime is not available.

0021-891X

Apart from the inherent technological advantages of maintenance-free operation, gelling affects the fundamental electrochemistry of the lead–acid batteries. Several recent studies [16–19] show that immobilization of the acid electrolyte influences the kinetic behaviour of both positive and negative electrodes apart from the minimization of acid stratification. For example, an analysis of the open-circuit potential transients as a function of state of charge shows substantial changes in the self discharge kinetics of the negative electrode as a result of gelling [16]. In addition, double layer capacitance (C_{dl}) and uncompensated resistance (R_u) measurements also reveal an enhancement of both the parameters in gelled electrolytes [17].

Although gelling induced effects on the kinetics of the $Pb/PbSO_4$ electrode have been recently studied, there is very little information regarding the effect on surface structure. Hence, the present study is aimed at understanding the effect of immobilization of the electrolyte on the surface structure of the negative electrode. In addition, effect of gelling on the kinetics of $Pb/PbSO_4$ electrode has been studied using a judicious choice of conventional electrochemical methods such as cyclic voltammetry, Tafel polarization and charging curve methods with modern surface spectroscopic techniques such as X-ray photoelectron spectroscopy (XPS) and scanning electron microscopy (SEM). The results of such studies are useful in understanding the effect of immobilization on the porous Pb electrode and thus in designing MF lead acid batteries.

2. Experimental details

Negative and positive pasted plates (5.5 cm × 3.0 cm × 0.1 cm) used in this study were obtained in cured and formed condition and the experimental details are described elsewhere [16]. In brief, negative limited test cells with excess sulfuric acid (4.8 M) electrolyte were assembled with two positive counter electrodes (PbO_2) arranged on both sides of the working electrode along with a Hg/Hg_2SO_4, H_2SO_4 (4.8 M) reference electrode. All the electrodes used in the present study were made with the same grid material namely Pb–Ca(0.08%)–Sn(0.5%) to preclude the possible effects of interaction by corrosion products of the grid. The reference electrode was connected to the test cell with a Luggin capillary tip aligned close to the working electrode to minimize the uncompensated resistance due to the solution.

2.1. *Cyclic voltammetric studies*

Cyclic voltammetric experiments were carried out in 0.1 M sulfuric acid solution using a lead electrode of geometric area 0.02 cm^2 in a three-electrode single compartment setup with a Hg/Hg_2SO_4, H_2SO_4 reference electrode and a platinum foil counter electrode. All the experiments were conducted using a PAR 173 potentiostat coupled with a PAR 175 function generator and the data were recorded on a RE0091 X–Y recorder in an argon atmosphere at a temperature of 25 ± 1 °C controlled by a thermostat. The experiments were then repeated with an immobilized electrolyte having the same sulfuric acid concentration. The latter was prepared by adding sodium silicate as gelling agent (5 g dm^{-3}) [20].

2.2. *Tafel polarization studies*

Tafel polarization was carried out using PAR 173 galvanostat. Prior to the measurements, the working electrode compartment was deaerated in the cell with pure argon, and the working electrode was then introduced immediately and kept at a current density of 1 A cm^{-2} from the moment of insertion in the electrolyte to prevent spontaneous corrosion, that is, from creating a build up of Pb^{2+} ions in solution for 10 to 15 min. After this polarization treatment at high current densities the electrode was found to attain a stable open-circuit potential. The steady state potential for the highest current density was recorded first and subsequent steady state potential for other current densities were recorded in descending order by decreasing the current densities in steps. The experiments were repeated with gelled electrolyte.

2.3. *Charging curve methods*

Charging curve measurements [21] were carried out using similar electrodes used for CV and Tafel polarization measurements. The electrode was first cathodically polarized by using appropriate current densities to the potentials corresponding to the ideal polarized region (IPE) of lead in sulfuric acid as obtained from the CV results. Potential build up with time was recorded for smallest current density and (dE/dt) was calculated from the slope of E/t curves with extrapolation to zero time. The experiments were then repeated with gelled electrolytes.

2.4. *Scanning electron microscopy*

Scanning electron micrographs of the lead electrode from completely discharged and overcharged cells were taken in a Leica Cambridge Stereoscan 440 model (M/S Leica, Cambridge, UK). The samples were mounted on a standard specimen mounting stub and then coated by a conducting thin layer of gold by vacuum deposition to prevent charging of the specimen. For comparative study, the electron beam parameters were kept constant while analysing all the lead samples. The micrographs of the samples with 10 kV EHT and 200 nA beam current were recorded by a 35 mm camera attached on the high resolution recording unit.

2.5. *X-ray photoelectron spectroscopy*

X-ray photoelectron spectroscopy (XPS) of the porous lead electrode from fully discharged and fully charged state with free and gelled electrolyte were carried out in a V.G. Scientific ESCA-3-MK2 elec-

tron spectrometer with MgK_α X-ray source (non-monochromatic). For the present measurements the anode was operated at a constant pass energy of 50 eV. All the spectra were recorded with similar spectroscopic parameters. The binding energy scale was calibrated by determining the binding energy of Au $4f_{7/2}$ (84 eV), Ag $3d_{3/2}$ (368.4) and Cu $2p_{3/2}$ (932.4) levels using spectroscopically pure metals from Johnson-Matthey, London. The binding energy values (measured to an accuracy of 0.2 eV) were in good agreement with literature values. The resolution in terms of the full width at half maximum (FWHM) of the Au $4f_{7/2}$ level was 1.6 eV.

3. Results and discussion

3.1. *Cyclic Voltammetric studies*

Figure 1 represents typical cyclic voltammograms of lead electrode in sulfuric acid with and without immobilization of the electrolyte at a representative scan rate of 10 mV s^{-1}. A comparison of the two voltammograms indicates a drastic change in the electrochemical behaviour of lead as a result of immobilization of the electrolyte. More specifically, the peaks for both lead dissolution (−950 mV) and deposition (−1000 mV) are flattened while the peak currents are increased in the gelled electrolyte and these effects are more pronounced for the deposition peak. The onset of HER is shifted by 700 mV cathodically as a result of gelling (−1.5 to −2.2 V). In addition, there is a small anodic peak for voltammograms with gelled electrolyte, possibly arising from the adsorbed hydrogen as the peak height is found to increase by holding the potential at the HER region for a few seconds and also since this is not observed at high scan rates.

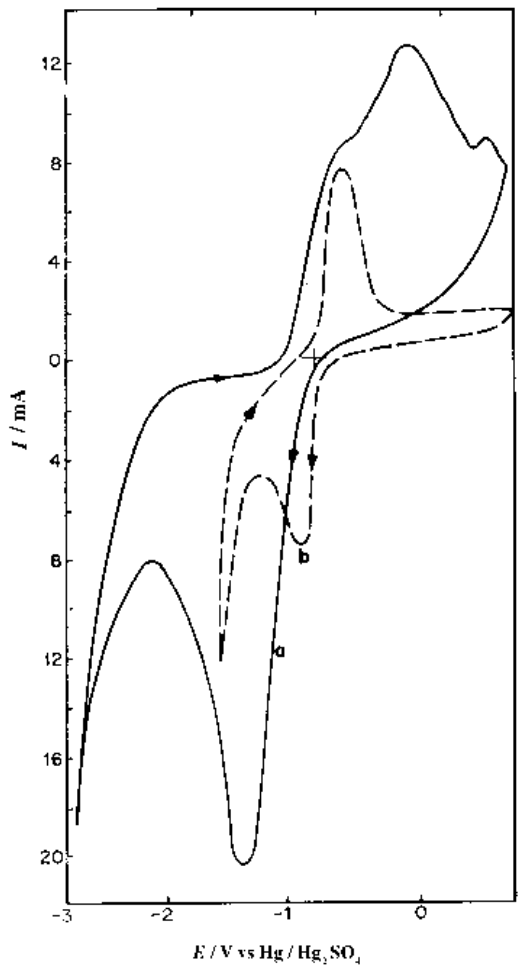

Fig. 1. Cyclic voltammograms of lead electrode (0.02 cm^{-2}) in sulfuric acid (0.1 M) at a scan rate of 10 mV s^{-1} with (a) and without (b) immobilization of the electrolyte in a potential region of −3 to + 0.5 V.

To avoid the formation of insoluble $PbSO_4$ and also to eliminate the complication from adsorbed hydrogen, the anodic and cathodic limit of the CVs were fixed at −0.8 V to −1.2 V, respectively, for further experiments. The typical cyclic voltammograms thus obtained for gelled and nongelled electrolyte at a scan rate of 10 mV s^{-1} are shown in Fig. 2(a) and (b) where the distortion due to gelling is particularly prominent. Interestingly, lead dissolution peak is shifted from −956 mV to −856 mV as a result of gelling while reduction peak is shifted from −1000 mV to −1044 mV. A major contribution to this shift is *IR* drop as evidenced by a 40 Ω increase in the internal resistance of the cell with the addition of gelling agent. This increased internal resistance can approximately shift the reduction potential cathodically by 40 mV (for 1 mA current). This is in further agreement with the flattening of the wave observed in the gelled electrolyte as the peak widths for both lead deposition and dissolution are increased. For example, ΔE_p of the cathodic peak is increased from 8 to 48 mV by immobilization (at the scan rate of 10 mV s^{-1}) while the anodic peak is expanded from 20 to 48 mV in the gelled electrolyte. The influence of gel is more pronounced in the case of the reduction peak as the species from the solution diffuses to the electrode surface and deposits there. This process is more influenced by the gel due to nucleation than the anodic process in which the dissolution is from the electrode surface.

Figure 3 shows the comparison of the anodic peak current variations with square root of scan rate in nongelled and gelled electrolyte, respectively. There is a drastic enhancement in the peak current magnitude as a result of gelling in spite of the slower diffusion and this increase is significantly more for the anodic peak than the cathodic one (not shown in Figure) in the gelled electrolyte. For example, at a scan rate of 10 mV s^{-1} $I_{p,a}$ is increased from 136 to 900 mA while $I_{p,c}$ is increased from 30 to 48 mA in gelled electrolyte possibly due to the electrocatalytic effect of silicate ions. This is more significant since the ohmic drop due to gelling should cause a reduction in all peak currents.

3.2. *Charging curve studies*

The charging curve method is a standard procedure for estimating double layer capacitance of any elec-

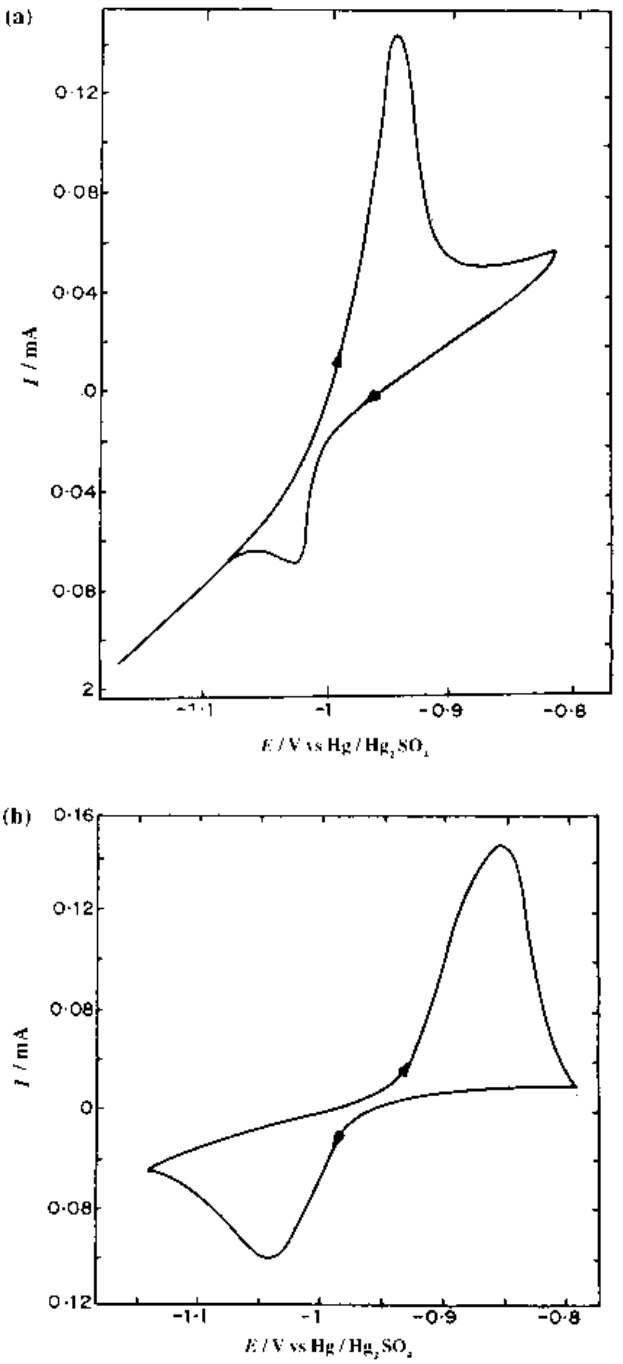

Fig. 2. Cyclic voltammograms obtained for (a) nongelled electrolyte and (b) gelled electrolyte at a scan rate of 10 mV s^{-1} in the region of −1.2 to −0.6 V.

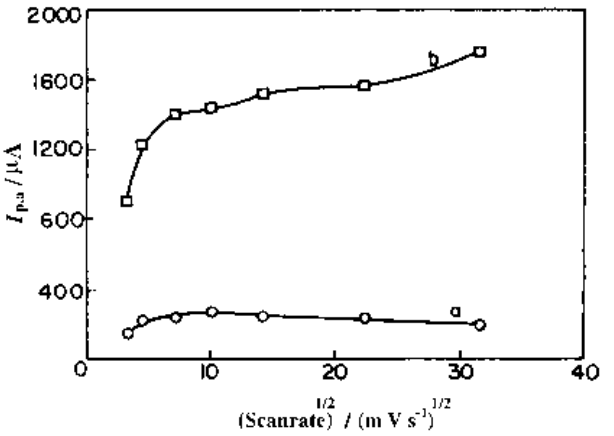

Fig. 3. Variation of anodic peak current with square root of scan rate in (a) nongelled and (b) gelled electrolyte, respectively.

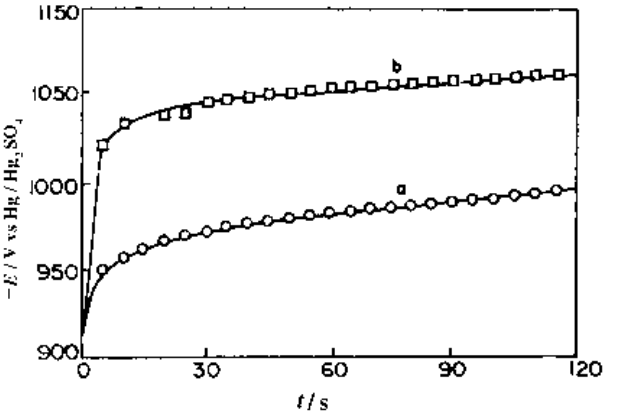

Fig. 4. Charging curve for the lead electrode in (a) free and (b) immobilized 1 M sulfuric acid electrolyte.

trode/electrolyte interface [21–23] in the ideal polarized region. The high hydrogen overpotential of lead facilitates the use of charging curve for the study of lead electrode/sulfuric acid interface in a limited cathodic region. The observed charging curve for the free and immobilized electrolyte in this region is shown in Fig. 4, indicating that there is an over all increase in double layer capacitance as a result of immobilization. The corresponding C_{dl} values calculated using the geometric area of the electrode for the free and immobilized electrolyte are 1400 μF cm^{-2} and 2000 μF cm^{-2}, respectively. These values are very high compared to the capacitance values for normal electrode/electrolyte interface and anomalous values are attributed to the surface roughness factor [24, 25]. Since the lead electrode used for both cases have same size there is no reason for such a drastic change in surface roughness and, therefore, the result indicates that the double layer capacitance values are enhanced significantly in gelled electrolyte. This enhancement can be explained by the fact that the double layer is compact in the gelled electrolyte compared to the free electrolyte, due to the increased hindrance of charge separation from the adsorbed silicate network, leading to a pronounced Helmoltz type behaviour rather than diffused behaviour.

3.3. *Tafel polarization methods*

Steady-state, potentiostatic, cathodic Tafel polarization plots for the lead electrode in gelled and normal electrolyte (Fig. 5) are recorded in the descending order of current densities. The Tafel slopes are found to be 120 and 170 mV, respectively, for gelled and free electrolytes. The exchange current density $I_{0,H}$ for HER calculated from the intercepts on the basis of apparent geometric area are 1.35×10^{-3} mA cm^{-2} and 1.31×10^{-5} mA cm^{-2} for free and gelled electrolytes, respectively, showing that the gel suppresses HER. This is in complete agreement with the cyclic voltammetric studies where a 700 mV cathodic shift

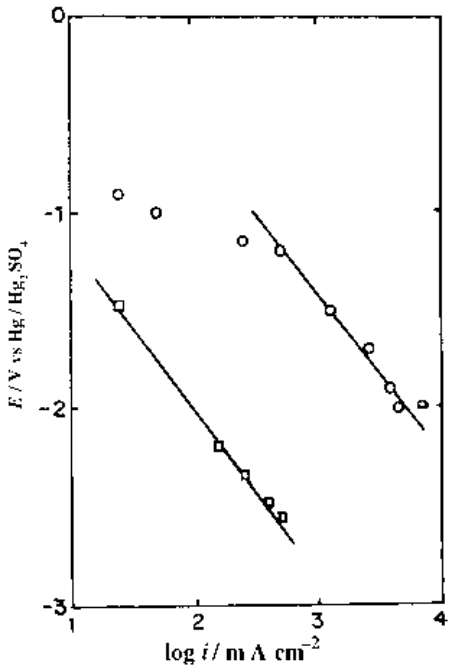

Fig. 5. Steady-state potentiostatic Tafel polarization curve in the cathodic region for (a) the free and (b) immobilized electrolyte.

is observed in HER as a result of immobilization. This suppression may be due to two major reasons: the gelling may affect the mass transfer of H^+ ions to the electrode surface by complexing of silicate ions and, more importantly, the silicate net work may change the surface properties of the lead electrode thereby, suppressing the chemisorption of protons at the lead electrode surface.

3.4. *Scanning electron microscopy*

Scanning electron micrographs of samples from overcharged and deeply discharged electrodes with and without immobilization of the electrolyte respectively are shown in Fig. 6(a)–(d). This clearly demonstrates the drastic effect of gelling on the morphology of lead electrode [26] both in the charged and discharged states. The SEM of the electrode from the fully charged state shows that the particles obtained in the case of gelled electrolyte are 10 times larger than that obtained from free electrolyte. This is mainly attributed to the effect of gelling on nucleation and growth involving Pb^{2+} ions in the solution as the growth rate depends on how fast the Pb^{2+} ions reach the electrode surface by diffusion. Gelling is known to control the nucleation and growth of crystals in other systems due to its unique control of viscosity. Gelling naturally hinders the rate of mass transfer to the electrode surface and in the free electrolyte the rate of nucleation is much faster. This, in turn, leads to the formation of a small number of big crystals rather than a large number of small crystals. In sharp contrast, micrographs of the electrode surface from the fully discharged electrodes indicate better dispersion due to gelling. The $PbSO_4$ particles are more finer in the case of gelled electrolyte and this may be the main reason for the enhanced utilization of the negative active material in gelled systems.

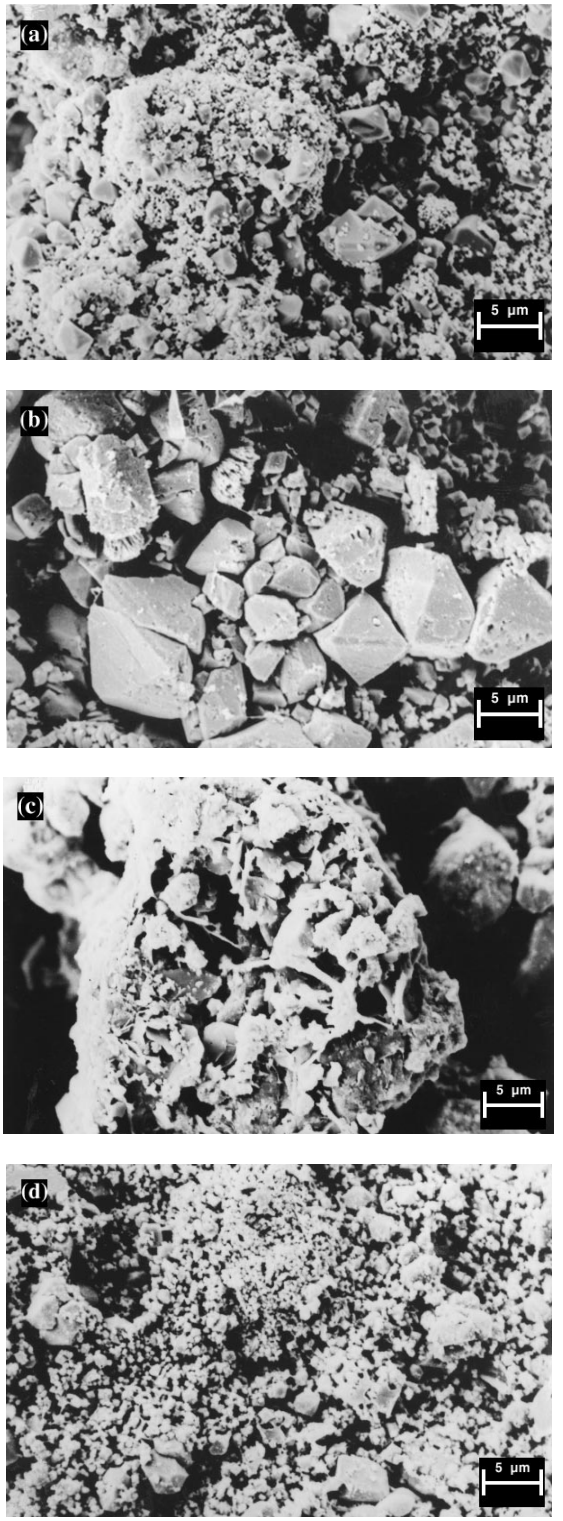

Fig. 6. Scanning electron micrographs for $Pb/PbSO_4$ electrodes from a fully charged cell (a,b) and fully discharged cell (c,d) with free and gelled electrolyte, respectively.

3.5. *X-ray photoelectron spectroscopy*

Significant changes in the surface morphology observed in gelled electrolyte, together with the substantial change in the fundamental electrochemistry of lead as a result of gelling, demands the char-

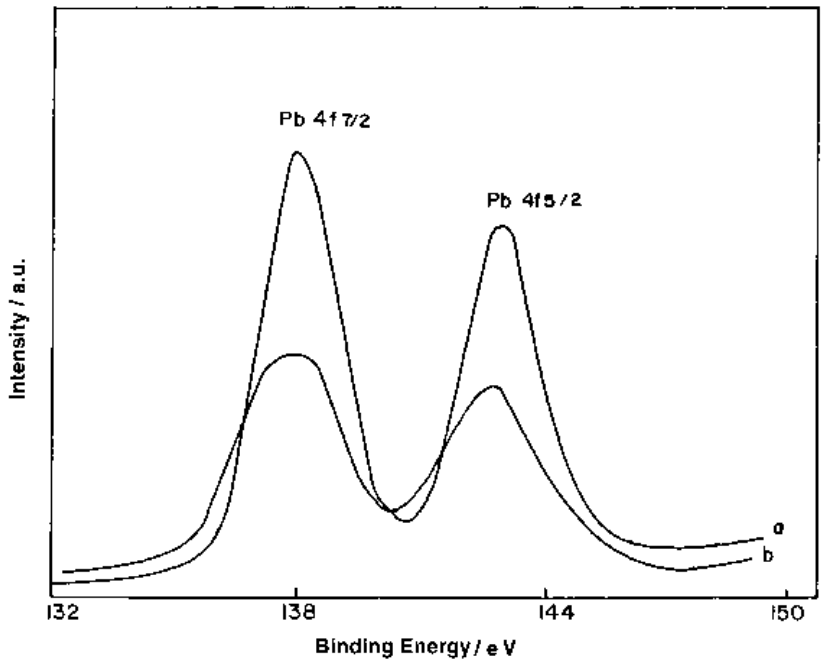

Fig. 7. Pb $4f_{7/2}$ and Pb $4f_{5/2}$ X-ray photoelectron spectra of lead electrode obtained from a fully discharged cell with (a) gelled electrolyte and (b) free electrolyte.

acterization of the surface composition by XPS. Chemisorbed species are in general [27] stable under the ultrahigh vacuum conditions used in the XPS measurements thus permitting their identification and if possible, quantification. The binding energy for Pb $4f_{7/2}$ and $4f_{5/2}$ signals corresponding to samples in the fully charged state are near 138.6 eV and are found to be insensitive to gelling although both signals for the fully charged electrode are found to be enhanced (Fig. 7). Significant change is not observed in the surface chemistry of lead in the gelled electrolyte. This is probably because the Pb–O–Si bond formed in solution may not be strong enough to withstand the ultrahigh vacuum conditions of the XPS spectroscopy. Similar results are also obtained for samples taken from a deeply discharged negative cell.

4. Conclusions

A combined application of cyclic voltammetry, charging curve methods and Tafel polarization along with XPS and SEM studies indicates a drastic change in the surface electrochemistry of lead as a result of the immobilization of the electrolyte. Although both lead deposition and dissolution become thermodynamically less favourable, the corresponding peak currents are interestingly enhanced with immobilization. Double-layer capacitance measurements, using the charging curve method, show that a major contribution of this increase is from the change in the interfacial structure. Tafel polarization studies prove that the HER reaction is suppressed by the addition of silicate and this is further confirmed by the cyclic voltammograms, where a 700 mV cathodic shift in HER is observed as a result of immobilization. SEM studies indicate a drastic change in morphology of the porous $Pb/PbSO_4$ electrode surface as a result of gelling, although XPS studies give no clear proof for the chemisorption of silicate ions on the lead electrode surface. These results may be important in understanding the operations of sealed MF lead–acid batteries.

References

[1] A. E. Alexander and P. Johnson, 'Colloid Science', Clarendon Press, Oxford (1949).
[2] I. C. Kwon, Y. H. Bae and S. W. Kim, *Nature* **354** (1991) 291.
[3] E. Tschida and K. Abe, *Adv.Polym.Sci.* **45** (1982) 1.
[4] K. Ignatova and J. Nikolova, *Bull. Electrochem.Soc.* **8** (1992) 266.
[5] G. Daccord and R. Lenormand, *Nature* **325** (1987) 41.
[6] J. Nittmann, G. Decord, H. E. Stankey., *ibid.* **314** (1985) 141.
[7] L. Nilemeyer, L. Pietronero and H. J. Weismann, *Phys. Rev. Lett.* **52** (1984) 1033.
[8] N. P. Pavletich and C. O. Paboo, *Science* **252** (1991) 809.
[9] R. Newmann and L. E. Michael, *Appl. Cat. A* **122** (1995) 85.
[10] R. G. Lindford (ed.), 'Electrochemical Science and Technology of Polymers' vols. **1–2**, Elserveir Applied Sciences, New York, (1987).
[11] M. E. Armand, J. J. Chabagno and M. J. Duclot., 'Fast Ion Transport in Solids' (edited by P. Vashishta, J. N. Mundy and G. K. Shenoy), North-Holland, Amsterdam (1979).
[12] M. T. Reetz, A. Zonta and J. Simpelkamp., *Angew. Chem. Int. Ed. Engl.* **34** (1995) 301.
[13] K. Vijayamohanan, S. N. Joshi and S. S. Sathayanaryana, *J. Power Sources* **30** (1990) 169.
[14] H. Tuphron, *ibid.* **23** (1988) 143.
[15] G. Posch, *ibid.* **33** (1991) 127.
[16] M. P. Vinod, and K. Vijayamohanan, *J.Appl. Electrochem.* **24** (1994) 44.
[17] Idem, *J. Power Sources* **50** (1994) 67.
[18] Idem, *J. Appl. Electrochem.* **25** (1995) 80.
[19] Idem, *J. Power Sources* **50** (1994) 67.
[20] R. Iler, 'The Chemistry of Silica', John Wiley, New York, (1979), p. 287.
[21] P. Delahay 'Double Layer and Electrode Kinetics', Wiley-Interscience New York (1965), Chapter 2.

[22] C. H. Preshred Jr. and S. Schuldimer, *J. Electrochem. Soc.* **180** (1961) 985.
[23] P. E. Bowden, *Proc. Roy. Soc.* **125A** (1929) 446.
[24] R. Delevie, *Adv. Electrochem. Engng.* **6** (1967) 239.
[25] J. Newman and W. Tiedemann, *AIChE J.* **21** (1975) 35.
[26] D. Pavlov and Z. Dinev, *J. Electrochem Soc.* **127** (1980) 885.
[27] A. T. Hubbard, *Langmuir* **6** (1990) 97.